Robust control and loop shaping design with the application to flexible rotor levitated with AMBs

Goranka Štimac[a], Sanjin Braut[a], Roberto Žigulić[a], Ante Skoblar[a]

[a] Faculty of Engineering, University of Rijeka, Vukovarska 58, 51000 Rijeka, Croatia, gstimac@riteh.hr

***Abstract*— The aim of this research is to ensure stable operation at a nominal rotation speed (above the first critical speed) of a flexible rotor levitated with active magnetic bearings (AMBs) and to guarantee good performance of the rotor/AMB system. Initially, minimizing the ITAE performance index, PID control system is designed to stabilize the rotor. The obtained transfer function is adopted as a compensator to shape the singular values of the nominal plant. By applying the Glover-McFarlane control method, a robust controller which includes coprime factor uncertainties is designed. The results show that the AMB system satisfies Zone A specifications defined by the ISO 14839 standard for newly commissioned machines with magnetic bearings.**

I. INTRODUCTION

Flexible rotors supported by active magnetic bearings (AMBs) are characterized by multiple lightly damped bending modes below the operating speed or within the controller bandwidth. Consequently, control of flexible rotors presents a challenge since linear design approaches are inherently only approximations of nonlinear dynamics [1]. Therefore, since PID control laws largely ignore model uncertainty and the coupled dynamics, they cannot guarantee robust stability and performance of rotor/AMB systems [2]. However, modern robust and optimal control theories provide a systematic method to optimize stability and performance of rotor/AMB systems [3].

Regarding the H_∞ robust method, two basic approaches can be distinguished, an approach based on the loop shaping and an approach based on the signals. Glover-McFarlane H_∞ method [4] is an open loop shaping method which has found its application in the field of AMBs as well [5, 6]. The main idea behind the loop-shaping in the open loop is that the singular values of the closed loop transfer function matrices can be determined directly from the singular values of the open loop system.

This paper focuses on the robust controller design for a flexible rotor/AMB system using the procedure as presented by Glover and McFarlane. The design procedure combines the loop shaping techniques from classical control with H_∞ synthesis so as to optimize the robustness against coprime factor uncertainty. In the first step, PID controller is designed to stabilize the rotor. In the second step, the singular values of the nominal plant are shaped by implementing the obtained PID controller model as a pre-compensator and the robust controller is designed by applying the Glover-McFarlane control method.

II. MATHEMATICAL MODEL

Fig. 1 presents the considered rotor/AMB system configuration. It consists of the flexible rotor levitated by two radial AMBs with non-collocation. The mass of each AMB rotor part is 8 kg. The length and the diameter of the shaft are 1.1 m and 0.025 m, respectively. Both AMBs operate with 0.3 mm radial air gap. In addition, three discs of the same dimensions (0.22 m in diameter and 0.05 m wide) are mounted on the shaft.

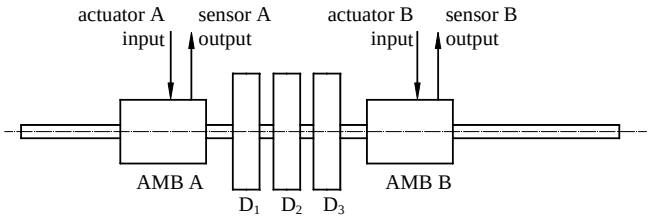

Figure 1. Flexible rotor/AMB system configuration, with three discs D_1, D_2 and D_3

By using the data from the finite element analysis, a structural mathematical model of the flexible rotor/AMB system in the modal coordinates can be constructed [7]. A nominal model **G** is defined as a state-space model described by the matrices **A**, **B**, **C** and **D**, as follows:

$$\begin{aligned}\mathbf{A} &= \begin{bmatrix} \mathbf{0} & \mathbf{I} \\ -\tilde{\mathbf{K}} + \mathbf{\Phi}^{\mathrm{T}}\mathbf{K}_{\mathrm{s}}\mathbf{\Phi} & -\tilde{\mathbf{D}} \end{bmatrix} \\ \mathbf{B} &= \begin{bmatrix} \mathbf{0} \\ \mathbf{\Phi}^{\mathbf{T}}\mathbf{K}_{\mathrm{i}} \end{bmatrix} \\ \mathbf{C} &= \begin{bmatrix} \mathbf{T}_{\mathrm{S}}\mathbf{\Phi} & \mathbf{0} \end{bmatrix} \\ \mathbf{D} &= \begin{bmatrix} \mathbf{0} \end{bmatrix}\end{aligned} \tag{1}$$

with

$$\begin{aligned}\tilde{\mathbf{D}} &= \mathrm{diag}\left(2\zeta_1\omega_1 \quad 2\zeta_2\omega_2 \quad \cdots \quad 2\zeta_{\mathrm{i}}\omega_1\right) \\ \tilde{\mathbf{K}} &= \mathrm{diag}\left(\omega_1^2 \quad \omega_2^2 \quad \cdots \quad \omega_1^2\right)\end{aligned}, \tag{2}$$

where ω_{i} and ζ_{i} are the natural frequency and the modal damping ratio of the *i*-th vibration mode. Furthermore, $\mathbf{\Phi}$ is the modal matrix of the mass normalized eigenvectors, $\mathbf{K}_{\mathrm{s}}$ and $\mathbf{K}_{\mathrm{i}}$ are 4×4 diagonal matrices of the force-displacement coefficients k_{s} and the force-current coefficients k_{i}, and $\mathbf{T}_{\mathrm{S}}$ is the Boolean matrix transforming the displacement outputs at

the corresponding degrees of freedom. The obtained natural frequencies of the flexible rotor model are: ω_1 = 266 rad/s, ω_2 = 729 rad/s and ω_3 = 1346 rad/s. The corresponding modal damping is 0.02, 0.01 and 0.005, respectively. In order to show rotor behavior at the AMB locations, the mode shapes (1st, 2nd and 3rd) of the system are shown in Fig 2.

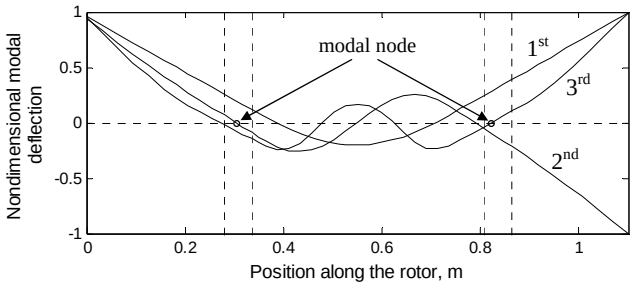

Figure 2. The natural mode shapes (1st, 2nd, 3rd) of the rotor/AMB system

The power amplifiers used to drive the actuator coils are modeled as a second order filter, with the cut-off frequency f_{amp} = 700 Hz and the damping ratio ζ_{amp} = 0.85. The position sensors are modeled as a simple constant K_{sens} = 8000 V/m. Moreover, the total phase delay due to unmodeled dynamics of the sensors and other electronic devices, including sampling time of the digital controller is modeled as a total time delay of 1.3 ms using the Padé approximation of the first order.

Finally, Figs. 3 and 4 show frequency response plots of the AMB A and AMB B from power amplifier inputs to position sensor outputs in *y*-axis.

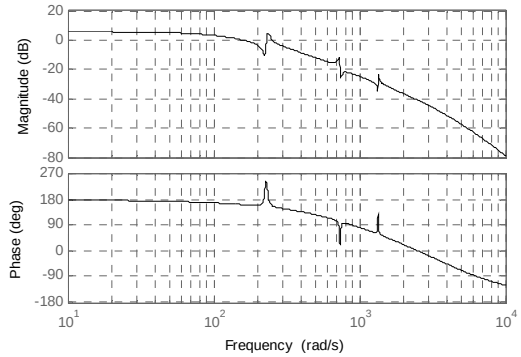

Figure 3. Frequency response plot of AMB A in *y*-axis

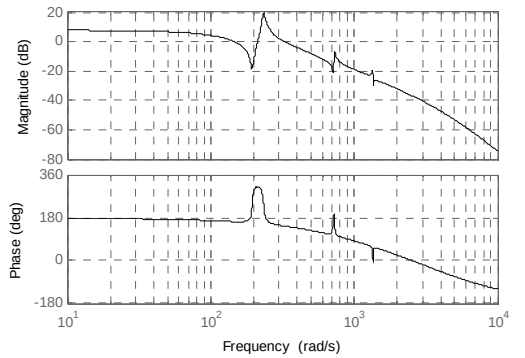

Figure 4. Frequency response plot of AMB B in *y*-axis

In Fig. 3 (at the 2nd bending mode of AMB A) and in Fig. 4 (at the 3rd bending mode of AMB B) it can be noticed that the pole appears before the corresponding zero. This indicates that the applied force at the near resonant rotor speeds would be 180° out of phase with respect to the measured displacement and special attention should then be paid to the controller design. Such observations are in accordance with the modal nodes position (Fig. 2).

III. CONTROL

A. PID control and gain optimization

A practical PID controller is characterized by the transfer function:

$$G_{pid} = K_p + \frac{K_{int}}{s} + K_d \frac{N_f}{1 + N_f / s}, \qquad (3)$$

where K_p is the proportional gain, K_{int} is the integral gain, K_d is the derivative gain and N_f is the filter coefficient. In order to define the set of parameters (K_p, K_{int}, K_d, N_f) the closed loop system structure of the system presented in Fig. 5 is adopted for controller tuning.

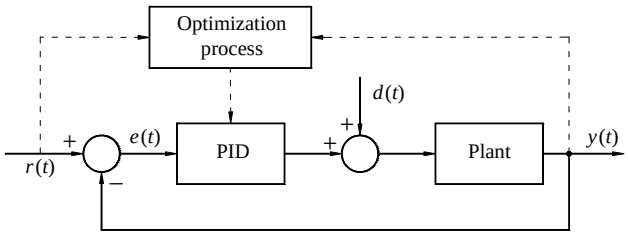

Figure 5. System structure adopted for PID controller tuning

Output response $y(t)$ of the system is compared with the desired response $r(t)$ and the resulting error $e(t) = r(t) - y(t)$ is minimized through an optimization performance criterion to determine the optimal PID gains. Here, the minimization of the integral of time multiplied by the absolute value of error (ITAE) is adopted, which is defined as:

$$J\left(K_p, K_{int}, K_d, N_f\right) = \sum_{i=1}^{m} \int_0^T t \left| e_i(t) \right| \mathrm{d}t, \qquad (4)$$

where T is the time of integration and $m = 4$ is the total number of control axes (two per one AMB), i.e. PID controllers.

The search of the PID controller design may be stated as a constrained multivariable optimization problem defined as:

$$\begin{aligned} &\min_x J(x) \text{ subject to } x > 0, \text{ where} \\ &x = \left[K_p, K_{int}, K_d, N_f\right] \end{aligned} \qquad (5)$$

For the minimization of the performance index (4), with the constraints defined in (5), built-in function *fmincon* of the Matlab Optimization Toolbox is used by applying the interior-point algorithm.

B. Glover–McFarlane H_∞ loop-shaping design procedure

The loop shaping procedure includes two steps. In the first step, the nominal model **G**, given in the form of its left

coprime factorization is shaped using the pre-compensator matrix $\mathbf{W}_1$ and the post-compensator matrix $\mathbf{W}_2$ (Fig. 6), so as to obtain the shaped plant:

$$\mathbf{G}_s = \mathbf{W}_2 \mathbf{G} \mathbf{W}_1 . \quad (6)$$

In the second step, robust stabilization of the shaped plant with respect of the coprime factor uncertainties is performed by synthesizing a stabilizing controller $\mathbf{K}_s$ [8]. The final controller can be then constructed by combining $\mathbf{K}_s$ with $\mathbf{W}_1$ and $\mathbf{W}_2$, such that

$$\mathbf{K} = \mathbf{W}_1 \mathbf{K}_s \mathbf{W}_2 . \quad (7)$$

An important advantage of the presented method is that it does not require explicit definition of uncertainties.

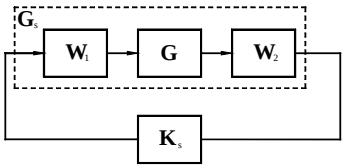

Figure 6. Shaped model $\mathbf{G}_s$ with controller $\mathbf{K}_s$

C. Compensator selection

The diagonal elements of $\mathbf{W}_1$ and $\mathbf{W}_2$ are selected so as to provide the desired shape of the singular values of the open-loop frequency response. However, in many practical applications, including AMBs, systems are unstable and can possess more than one gain crossover frequency. In such cases, the selection of the transfer functions for the design of the open loop process becomes difficult.

In this paper it is shown that $\mathbf{W}_1$ can be efficiently selected as the following diagonal transfer function matrix:

$$\mathbf{W}_1 = \begin{bmatrix} w & 0 & 0 & 0 \\ 0 & w & 0 & 0 \\ 0 & 0 & w & 0 \\ 0 & 0 & 0 & w \end{bmatrix}, \quad w = G_{\text{pid}} G_{\text{notch2}} G_{\text{notch3}} , \quad (8)$$

where G_{pid} is the PID controller transfer function defined in (3) and G_{notch2} and G_{notch3} are the notch filters related to the 2nd and the 3rd bending modes defined as:

$$G_{\text{notch2}} = \frac{s^2 + \omega_{\text{notch2}}^2}{s^2 + 2\zeta_{\text{notch2}}\omega_{\text{notch2}} s + \omega_{\text{notch2}}^2}, \quad G_{\text{notch3}} = \frac{s^2 + \omega_{\text{notch3}}^2}{s^2 + 2\zeta_{\text{notch3}}\omega_{\text{notch3}} s + \omega_{\text{notch3}}^2} \quad (9)$$

The corresponding central frequencies of the notch filters are ω_{notch2} and ω_{notch3} and the corresponding damping ratios are ζ_{notch2} and ζ_{notch3}. Controller parameters (K_p, K_{int}, K_d, N_f) are obtained by minimization of ITAE performance index (4).

Since in the observed AMB system there is no difference between importance of the outputs, $\mathbf{W}_2$ is selected as 4×4 unit diagonal matrix.

IV. SIMULATION RESULTS AND CONCLUSION

This chapter presents an analysis of the closed loop sensitivity functions of the rotor/AMB system, referring to the ISO 14839-3 standard [9]. From the measured sensitivity function $S(j\omega)$ of each control axis ($i=1,\ldots,m$) in the frequency domain, the index to be evaluated is obtained from the relationship:

$$S_{\max} = \max_i \left[\max \left| S(j\omega) \right| \right], \quad 0 \le \omega \le 2\pi f_{\max} , \quad (10)$$

where $f_{\max}$ is the maximum frequency in the observed frequency range. Equation (10) generally states that the overall system rating is determined as the worst rating of any of the transfer functions individually measured for all four control axes.

The Glover–McFarlane H_∞ loop-shaping controller design procedure was carried out for the rotational speed Ω = 30 Hz (subcritical speed). Figs. 7 – 14 show plots of output sensitivity of the rotor/AMB system for the *y*-axis of AMB A and *y*-axis of AMB B for both PID and robust control methods. The magnitudes are measured at standstill (Ω = 0 rad/s), at Ω = 30 Hz (188.5 rad/s), at Ω = 50 Hz (314.2 rad/s) and at Ω = 60 Hz (377 rad/s). The presented results are obtained with the following parameters: K_p = 0.6393, K_{int} = 6.271, K_d = 0.004, N_f = 80000, ω_{notch2} = 729 rad/s, ω_{notch3} = 1346 rad/s and ζ_{notch2} = ζ_{notch3} = 0.15.

Since the output sensitivity function provides a means of quantifying the disturbance rejection of the closed loop system, it can be concluded that the AMB system controlled by the proposed algorithm (PID + Glover-Mcfarlane) provides better disturbance rejection property than the system controlled solely by PID. Moreover, peak sensitivity lower than 3 (in absolute terms) satisfies *Zone* A specifications for newly commissioned machines with magnetic bearings defined by ISO 14839-3 and, therefore, indicates very good stability margin (as in Figs. 7 – 11). *Zone* B (peak sensitivity from range 3 – 4) is normally considered acceptable for unrestricted long-term operation (as in Figs. 12 and 13). However, maximal magnitude of the output sensitivity for AMB B at Ω = 60 Hz (as in Fig. 14) is equal to 5.38, indicating very poor stability margin (*Zone* D). This peak corresponds to excitation of the 2nd bending mode of the rotor which introduces non-collocation into the system (pole before zero at the 2nd bending mode of AMB A, Fig. 3).

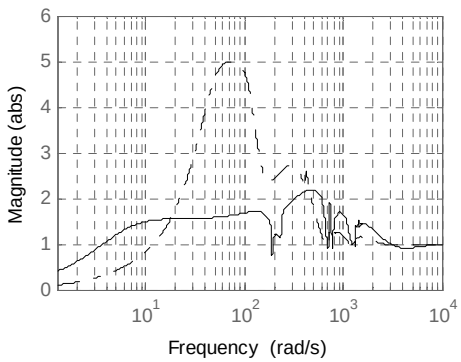

Figure 7. Output sensitivity function of the AMB A (Ω = 0 rad/s); PID(–.), PID+Glover-McFarlane (—)

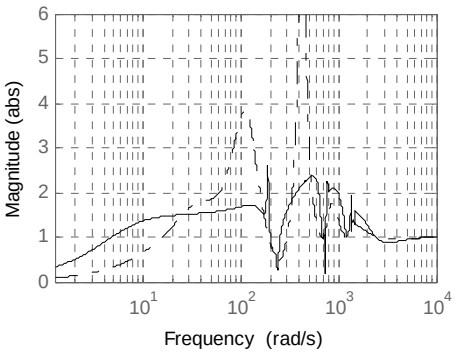

Figure 8. Output sensitivity function of the AMB B (Ω = 0 rad/s); PID(–.), PID+Glover-McFarlane (—)

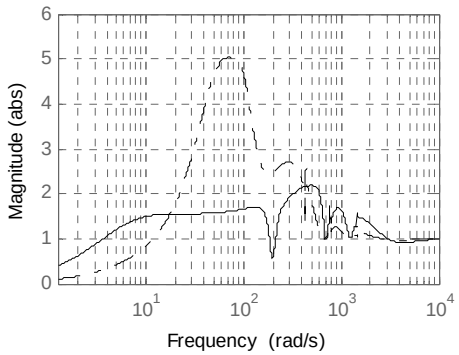

Figure 9. Output sensitivity function of the AMB A (Ω = 188.5 rad/s); PID(–.), PID+Glover-McFarlane (—)

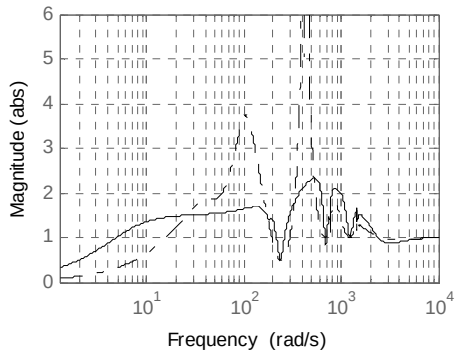

Figure 10. Output sensitivity function of the AMB B (Ω = 188.5 rad/s); PID(–.), PID+Glover-McFarlane (—)

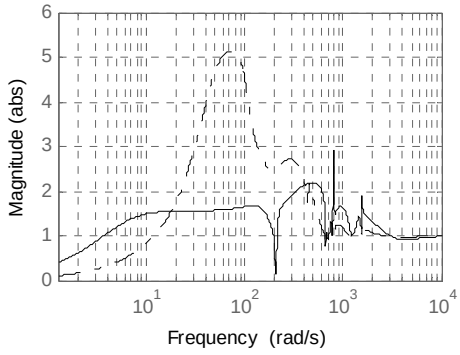

Figure 11. Output sensitivity function of the AMB A (Ω = 314.2 rad/s); PID(–.), PID+Glover-McFarlane (—)

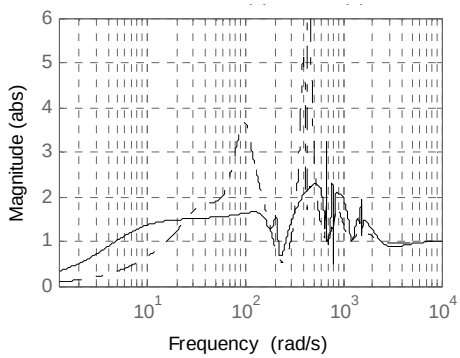

Figure 12. Output sensitivity function of the AMB B (Ω = 314.2 rad/s); PID(–.), PID+Glover-McFarlane (—)

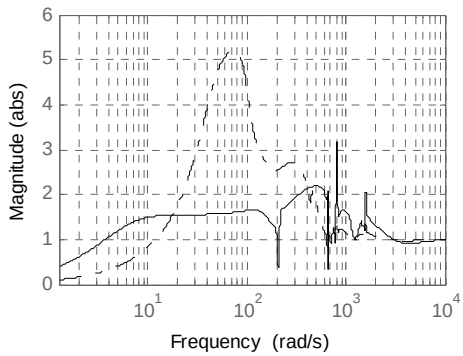

Figure 13. Output sensitivity function of the AMB A (Ω = 377 rad/s); PID(–.), PID+Glover-McFarlane (—)

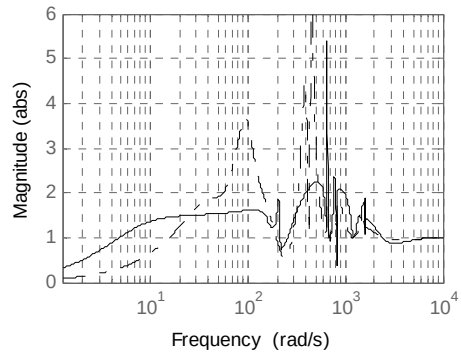

Figure 14. Output sensitivity function of the AMB B (Ω = 377 rad/s); PID(–.), PID+Glover-McFarlane (—)

In conclusion, the proposed procedure does not satisfy the ISO standard in the entire frequency range if the non-collocation problem exists. However, with no collocation problems it provides stable operation of the flexible rotor/ AMB system above the first critical speed.

ACKNOWLEDGEMENT

Research reported in this paper was supported by University of Rijeka, Croatia Grants No. 13.09.1.2.11 and No. 13.09.2.2.19.

REFERENCES

[1] G. Balas, J. Doyle, "Robustness and performance trade-offs in control design for flexible structures," *IEEE Transactions on Control System and Technology*, vol. 2, no. 4, pp. 352-361, 1994.

[2] S. E. Mushi, Z. Lin, P. E. Allaire, "Design, construction and modeling of a flexible rotor active magnetic bearing test rig," *IEEE/ASME Transactions on Mechatronics*, vol. 17, no. 6, pp. 1170-1182, 2012.

[3] K. Zhou, J. Doyle, "Robust and Optimal Control," Prentice-Hall, Upper Sadle River, New Jersey, 1996.

[4] K. Glover, D. McFarlane, "Robust stabilization of normalized coprime factor plant descriptions with H_∞ bounded uncerainty," *IEEE Transations on Automatic Control*, vol. 34, pp. 821–830, 1989.

[5] A. L .F. Driemeyer, H. Bourles, E. R. De Pieri, "A robust nonlinear controller with application to a magnetic bearing system," *Proceedings of the 44th IEEE Conference on Decision and Control*, 2005, pp. 4927–4932, 2005.

[6] E. S. Armstrong, "Robust controller design for flexible structures using normalized coprime factor uncertainty," *NASA Technical Paper 3325*, Langley Research Center, Hampton, Virginia, 1993.

[7] G. Štimac, S. Braut, N. Bulić, R. Žigulić, "Modeling and Experimental Verification of a Flexible Rotor/AMB System," *COMPEL: The International Journal for Computation and Mathematics in Electrical and Electronic Engineering*, vol. 32, pp.1244-1254, 2013.

[8] S. Skogestad, I. Postlethwaite, "Multivariable feedback control," John Wiley & Sons, 1996.

[9] ISO 14839-3:2006, Mechanical vibration — Vibration of rotating machinery equipped with active magnetic bearings, Part 3: Evaluation